HHS Public Access

Author manuscript

Radiat Res. Author manuscript; available in PMC 2020 September 01.

Published in final edited form as:

Radiat Res. 2019 September ; 192(3): 267–281. doi:10.1667/RR15379.1.

Radioresistance of Serpinb3a–/– Mice and Derived Hematopoietic and Marrow Stromal Cell Lines

Stephanie Thermozier[a], **Xichen Zhang**[a], **Wen Hou**[a], **Renee Fisher**[a], **Michael W. Epperly**[a], **Bing Liu**[b], **Ivet Bahar**[b], **Hong Wang**[c], **Joel S. Greenberger**[a,1]

[a]Department of Radiation Oncology, UPMC Hillman Cancer Center, Pittsburgh, Pennsylvania 15213;

[b]Department of Computational Biology, University of Pittsburgh, Pittsburgh, Pennsylvania 15260

[c]Department of Biostatistics, University of Pittsburgh, Pittsburgh, Pennsylvania 15260

Abstract

Serpins are a group of serine-proteases involved in multiple signal transduction pathways in mammalian cells. In particular, Serpinb3a is involved in the lysosomal necrosis cell death pathway with components that overlap with radiation-induced apoptosis. We investigated the radiation response of Serpinb3a$^{-/-}$ mice compared to Serpinb3a$^{+/+}$ mice on the Balb/c background. Serpinb3a$^{-/-}$ mice showed significant radioresistance to a dose of 8.0 Gy total-body irradiation, compared to Serpinb3a$^{+/+}$ Balb/c mice. Long-term bone marrow cultures from Serpinb3a$^{-/-}$ mice showed increased longevity. In clonogenic survival assays, fresh bone marrow hematopoietic progenitors, as well as clonal interleukin-3 (IL-3)-dependent hematopoietic progenitor and bone marrow stromal cell lines from Serpinb3a$^{-/-}$ mice were radioresistant. Serpinb3a$^{-/-}$ mouse bone marrow-derived stromal cell lines had increased baseline and postirradiation antioxidant capacity. Serpinb3a$^{-/-}$ bone marrow stromal cells showed increased radiation-induced RNA transcripts for MnSOD and p21, and decreased levels of p53 and TGF-β. Both irradiated Serpinb3a$^{-/-}$ mouse bone marrow stromal cell lines and plasma removed from total-body irradiated mice had decreased levels of expression of stress response and inflammation-associated proteins. Abrogation of Serpinb3a may be a potential new target for mitigation of radiation effects.

INTRODUCTION

Serpins are a family of serine protease inhibitors that serve a variety of biological roles (1–5), including inhibition of serine and cysteine protease activity, and regulation of proteolytic cascades leading to cell death (5–7). Over 1,500 serpin-like genes have been identified in multiple organisms ranging from viruses to archaea and plants (1). Serpins in eukaryotic cells are divided into 16 “clades” (labeled A–P) based on their phylogenetic relationship.

[1]Address for correspondence: Department of Radiation Oncology, UPMC Hillman Cancer Center, UPMC Cancer Pavilion, POB2, Rm. 533, 5150 Centre Avenue, Pittsburgh, PA 15232; greenbergerjs@upmc.edu.

Editor’s note. The online version of this article (DOI: 10.1667/RR15379.1) contains supplementary information that is available to all authorized users.

Some serpins have non-inhibitory functions including hormone transport as chaperone proteins, blood pressure regulators and tumor suppressors (8).

Serpins are designated by two letters, for example, SerpinXy where “X” is the clade and “y” is number within the clade (2). In addition to clades there are a number of “orphan” serpins not yet categorized, and some with alternative names based on their origin and their function (3). In humans, 36 serpins have been identified, 26 of which have inhibitory activity with respect to several signal transduction pathways. The complete activity and scope of interactions of most serpins are not yet understood (2–4).

The flatworm *C. elegans* was utilized to derive cell lines with selected deletion of specific serpins (6). These *C. elegans* strains were chosen as a model organism due to their limited repertoire of serpins, called SRP molecules, which are evolutionarily conserved. *C. elegans* strains with absence of the SRP-6 serpin showed lysosomal mediated cell death induced by hypoxia, hyperoxia, hypotonic and oxidative stress. Cell death in these null animals showed a necrotic phenotype that was attributed to the loss of cysteine peptidase inhibitory, which normally leads to expression of MEC-4, a degenerin/epithelial Na^+ channel that blocks necrosis (6). After induction of direct lysosomal injury with acridine orange and ultraviolet light, both wild-type and SRP-6 null *C. elegans* showed lysosomal disintegration; however, wild-type animals survived and reconstituted lysosomal integrity while SRP-6 null animals did not recover (6). Other genes implicated in apoptosis and autophagy in *C. elegans* were not specifically implicated, suggesting a novel cell death pathway mediated by SRP-6 (4, 5).

Many of the 13 human serpins in clade B are designated as secreted, but some are primarily intracellular because they lack a secretory signal peptide sequence. The clade B serpins have been implicated in regulatory processes including those in the immune system function, angiogenesis, coagulation and fibrinolysis (5). The intracellular location of clade B serpins has been hypothesized to serve a pro-survival function by limiting damage caused by lysosomal cysteine or serine peptidases (4, 5). The intracellular serpin B3/B4 ortholog (which in mice is Serpinb3a) has a pro-survival function by blocking damage induced by lysosomal proteases (7). The data also suggested a novel role of serpins in oxidative stress-induced cell death by lysosomal-mediated necrosis (6). In the current studies, we tested Serpinb3a$^{-/-}$ mice and derived cell lines compared to Serpinb3a$^{+/+}$, Balb/c background strain controls for radiation response. The results demonstrate an unexpected radioresistance of Serpinb3a$^{-/-}$ mice, as well as their derived hematopoietic and mesenchymal stem cell lines, and an overall reduced level of response to radiation-induced stress and inflammation.

MATERIALS AND METHODS

Mice and Animal Facilities

Serpinb3a$^{-/-}$ and Serpinb3a$^{+/+}$ mice derived on the Balb/c background were obtained from Charles River Laboratories (Wilmington, MA) with permission from Dr. Gary Silverman (University of Washington, St. Louis, MO). Female mice were housed 5 per cage and male mice housed 4 per cage according to Institutional Animal Care and Use Committee (IACUC) regulations. Mice were fed standard Purinat® 5001 laboratory chow. All protocols

were approved by the University of Pittsburgh IACUC. Veterinary care was provided by the Division of Laboratory Animal Resources at the University of Pittsburgh (Pittsburgh, PA).

Irradiation

Mice received either no radiation (not sham irradiated) or 8.0 Gy total-body irradiation (TBI) using a Shepherd Mark 1 ^{137}Cs gammaray source (9–12) (JL Shepherd, San Fernando, CA), at 320 cGy/ min, according to published methods (9). Mice were given hyperchlorinated water. In other experiments, animals were placed in the irradiator, but not irradiated (sham irradiated), and we detected no differences in the effect of TBI relative to "preirradiation" or sham irradiation (10). The 320 cGy/mm dose rate was used to limit animal time in the irradiator, and the lack of detectable biologic effect of this change in dose rate relative to the 70 cGy/min dose rate used previously has been published elsewhere (9). This dose rate is also in the range as that used to treat patients in clinical radiation therapy (approximately 200 cGy/min). Animals were irradiated in a rotating pie-shaped device containing 12 sections. One mouse was placed in a section with one or two empty sections left before the next mouse, so that 5 mice were irradiated in each pie-shaped device at each time. Radiation was delivered from one side by the cesium source. Three pie-shaped devices were stacked on top of each other and were irradiated at each session for a total of 15 mice per session. Animals were not restrained, and the same protocol was used for all sessions.

Long-Term Bone Marrow Cultures

Long-term bone marrow cultures (LTBMCs) were established, according to methods published elsewhere (10, 11), from the femur and tibia marrow of Serpinb3a$^{-/-}$ or Serpinb3a$^{+/+}$ mice on the Balb/c background. Briefly, the contents of a femur and tibia were flushed into McCoy's 5A medium (Thermo Fisher Scientifice™, Waltham, MA) supplemented with 25% horse serum (Cambrex, Rockland, ME) and 10^{-5} *M* hydrocortisone sodium hemisuccinate (Thermo Fisher Scientific). For each group, two mice were used to establish LTBMCs, and two flasks were created per mouse for a total of four cultures (one tibia and one femur marrow contents per flask, total of four per mouse genotype). This number is consistent with other laboratory-reported numbers, as well as our own previously published work (10, 11). Cultures were incubated at 33°C in 7% CO_2. Media was changed weekly. After 4 weeks, the horse serum was replaced with 25% FBS (Gemini Bio-Products, West Sacramento, CA) (10, 11). The cultures were observed weekly for hematopoietic cell production and adherent cell layer confluence. Nonadherent cell production data were expressed as mean ± standard error of the mean (SEM) of weekly nonadherent cell number and cumulative nonadherent cell production. (n = 4 flasks harvested per genotype.) Surface area confluence data were expressed as mean ± SEM of percentage of the adherent cell layer that showed confluent cells.

Hematopoietic Colony-Forming Cell Assay

Fresh marrow colony-forming assays were performed as described elsewhere (10). Each week after explant and establishment of LTBMCs, 1×10^5 nonadherent cells were plated in triplicate in 0.8% methylcellulose-containing media in plates, as described elsewhere (10). Cells were incubated in a high-humidity incubator at 37°C in 5% CO_2. At days 7 and 14 after plating, colonies of ≥50 cells were counted by inverted microscope. The plates that

were scored at day 7 were then returned to the incubator for scoring again at day 14. Data for days 7 and 14 colony numbers are presented as mean ± SEM of weekly colony-forming cells per 5×10^4 cells plated, n=4 plates per data point, and we also plotted cumulative production of colony-forming cells (10). The day 7 colonies represent more differentiated hematopoietic progenitor cells forming cells within each single cell colony, identifiable as granulocytes (neutrophils) and macrophages (colony-forming unit-granulocyte, macrophage; CFU-GM). The day 14 colonies (reaching ≥50 cells/colony between days 7–14) are representative of more primitive hematopoietic progenitors forming single cell-derived colonies consisting of erythroid, megakaryocyte, as well as granulocyte and macrophage lineages (colony-forming unit-granulocyte erythroid, macrophage, megakaryocyte; CFU-GEMM) (10).

Establishment of Bone Marrow Stromal Cell Lines

Adherent cell layers from one LTBMC per genotype group after week 20, when hematopoietic cell production had ceased, were trypsinized and expanded by passage in Dulbecco's modified Eagle's Medium (DMEM) supplemented with 10% FBS to establish bone marrow stromal cell lines according to methods published elsewhere (10). We used established criteria for authentication of bone marrow stromal cell lines including: positivity for alkaline phosphatase, collagens 1–4, production of TGF-β and production of macrophage colony stimulatory factor (10, 11). We performed genotyping of all bone marrow stromal cell lines that were established, and confirmed that they were from the Serpinb3a$^{-/-}$ or the control Serpinb3a$^{+/+}$ Balb/c background genotype. This genotyping procedure was done to ensure integrity of laboratory technique and quality control of standard procedures, not because the genotype was expected to change. The established cell lines were maintained *in vitro* by weekly passage at 1:4 and 1:10 dilutions, and retained stromal cell features including differentiation capacity to osteoblasts, and support of co-cultivated purified hematopoietic cells in co-culture (10). We documented cell surface phenotype, morphology and absence of capacity to differentiate to hematopoietic cells in the semisolid culture assay, described above, for days 7 and 14 CU-GM and CFU-GEMM, respectively. All cell lines were characterized as bone marrow stromal cells or mesenchymal stem cells using methods reported elsewhere (10, 11). Cell lines were incubated at 37°C in 5% CO_2 and passaged weekly for 10 weeks to establish permanent bone marrow stromal cell lines.

Establishment of Single Cell-Derived Clonal Marrow Interleukin-3-Dependent Hematopoietic Cell Lines

Single cell cloning experiments were performed using nonadherent cells from the harvest of one week 4 LTBMC from each genotype, as described elsewhere (10). Flow cytometry was used to plate single nonadherent cells into each well of a 96-well plate. Cells were grown in DMEM supplemented with 10% (Walter and Eliza Hall Institute) WEHI-3 cell line conditioned media, as a source of interleukin-3 (IL-3) (39), 20% FBS, 1% antibiotic-antimycotic solution and 1% L-glutamine. Plates were observed weekly for growth. Clonal lines were established from wells that showed growth after single cell plating. The clonal lines were expanded in media supplemented with 10 μl/ml mouse IL-3 (PeproTecht® Inc./ VWR® International, Radnor, PA). IL-3 independence of cell lines was tested, as an indication of malignant transformation (35, 36). We documented the absence of IL-3

independence by growing 10^5 cells per ml in media in the absence of added IL-3 and confirmed no growth. IL-3-dependent cell lines displayed cell death after 7 days in the absence of added IL-3. The majority of published IL-3-independent lines have been shown to form tumors *in vivo* and are radioresistant *in vitro* (35, 36).

Radiation Survival Curves

Radiation sensitivity of Serpinb3a$^{-/-}$ and Serpinb3a$^{+/+}$ Balb/c background cell lines was determined using radiation survival curves as previously described (10). Single cell suspensions were prepared from Serpinb3a$^{-/-}$ and Serpinb3a$^{+/+}$ Balb/c background freshly isolated bone marrow, IL-3-dependent cell lines and bone marrow stromal cells, and were irradiated with doses of 0–8 Gy at intervals of 1, 2, 3, 4, 5, 6, 7, 8 Gy. Cells were then plated in either semisolid media in 0.8% methylcellulose containing media or in 4-well flat bottom plates (39). Seven days later, colonies of >50 cells from the fresh bone marrow or IL-3-dependent cell lines were scored in methylcellulose containing media cultures. For the bone marrow stromal cell cultures, the plates were stained with crystal violet, and colonies of >50 cells were counted (10). All colony data were analyzed using linear quadratic or single-hit, multi-target models (10). In some experiments, with the bone marrow stromal cells, the small molecule radiation mitigator drugs, JP4–039 or necrostatin-1 (9), were each added at 10 mM 1 h before irradiation, and kept in media containing that drug continuously until the colonies were counted.

Polymerase Chain Reaction (PCR) for Detection of Serpinb3a

DNA was extracted using proteinase K and ethanol precipitation as previously described. PCR was performed using the following primers: b3a specific primer F (CAGATGATGAAACAAAACATCG), b3a specific primer R (AGACCTTGAGTGCTGCTCATA) and Neo F (CTTGGGTGGAGAGGCTATTC). PCR was performed using Promega GoTaqt® G2 DNA Polymerase (Madison, WI) and 1 μl of DNA. Cycling conditions were 95°C for 5 min followed by 35 cycles of 95°C for 40 s, 30°C for 40 s and 72°C for 1 min. This was followed by 72°C for 5 min and then incubation at 4°C (12, 13).

RT-PCR Detection of Inflammatory Cytokine and Stress Response Gene Transcripts

Quantitative reverse transcription polymerase chain reaction (qRTPCR) was performed for analysis of gene expression levels. Cell lines or tissue from each mouse was individually homogenized and RNA extracted using TRIzol® reagent (Invitrogen™, Carlsbad, CA). A total of 2 μg of RNA was used to synthesize cDNA in a 20 μl reaction, following the instructions of the High-Capacity cDNA Reverse Transcription Kit (Applied Biosystemst®, Carlsbad, CA). qRT-PCR reaction was performed using iTaq™ Universal Probes Supermix (Bio-Rad® Laboratories Inc., Hercules, CA), 40 cycles of 95°C (denaturation) for 15 s and 59°C (annealing and elongation) for 30 s using the Eppendorf RealPlex 2 Mastercycler® (Westbury, NY) (13).

The real-time polymerase chain reaction was used to measure radiation-inducible transcripts for: transcription factors NF-κβ, Ap1, Sp1 and Nrf2; cytokines including TGF-β1 and IL-1α; oxidative stress response enzyme MnSOD (Sod2); and radiation-response-related

transcripts (32). Results were standardized by comparison to glyceraldehyde-3-phosphate dehydrogenase (GAPDH). The results were shown as fold increase or decrease in gene transcript expression above baseline level, which was adjusted to that for nonirradiated wild-type-Balb/c mouse tissue or cell lines. Significance was determined to be that of a twofold or greater difference or less than 0.5-fold decreased difference.

The RT-PCR conditions were as follows: 96-well plates were prepared with 10 μl of iTaq™ Universal Probes Supermix (Bio-Rad), 5 μl of RNase-free water, 1 μl of the corresponding TaqMan Gene Expression probe, and 4 μl of cDNA (equivalent 0.1 μg of RNA) using the Eppendorf epMotion® 5070 automated pipetting system. PCR amplification of the GAPDH gene was used as the housekeeping gene. Expression of Nrf2, Sod2, NF-κβ, TGF-β1, Gadd45, IL1α, Sp1, Ap1, Rad51, p21, p53 and GAPDH was determined by RT-PCR. Gene bank numbers for each gene are shown in Supplementary Table S1 (http://dx.doi.org/10.1667/RR15379.1.S1) (13).

Western Blot for Analysis of Proteins

Western blot analysis of proteins was performed on tissues and cell lines. Explanted tissues were homogenized, and electrophoresis was performed on 15% polyacrylamide gels. The protein was transferred to a nitrocellulose membrane treated with antibodies as described, and quantitated as standardized to GAPDH (9, 13).

Luminex® Assay for Protein Quantitation in Cell Lines and Freshly Removed Mouse Tissues

Serpinb3a$^{-/-}$ or Serpinb3a$^{+/+}$ Balb/c background bone marrow stromal cells from cell lines irradiated *in vitro* were collected at 0, 1, 2, 3 or 24 h after 10 Gy irradiation. Fresh bone marrow and the (small intestine) ileum was harvested from Serpinb3a$^{-/-}$ and Serpinb3a$^{+/+}$ Balb/c background strain at days 0, 1, 3 or 5 after 8 Gy TBI and immediately frozen. The cells or tissues were thawed, homogenized in0.1% Tween™ 80 in phosphate buffered saline (PBS; Thermo Fisher Scientific, Waltham, MA) and protein quantitated using Bio-Rad Protein Assay (Hercules, CA). The ileum was thawed, and a 4 mg piece was homogenized in 1 ml of 0.1% Tween 80 in PBS and protein quantitated using Bio-Rad Protein Assay (9). A 32 Multiplex Mouse Cytokine/Chemokine Magnetic Bead Panel (EMD Millipore, Billerica, MA) was used to measure protein concentrations for eotaxin, G-CSF, GM-CSF, IFN-γ, IL-1α, IL-1β, IL-2, IL-3, IL-4, IL-5, IL-6, IL-7, IL-9, IL-10, IL-12 (p40), IL-12 (p70), IL-13, IL-15, IL-17, IP-10, KC, LIF, LIX, MCP-1, M-CSF, MIG, MIP-1α, MIP-1β, MIP-2, RANTES, TNF-α, and VEGF. TGF-β concentrations were measured using a TGFBMAG-64K-01kit (EMD Millipore). A MAGPIX® instrument (Millipore Sigma, Burlington, MA) was used to run the assays (9).

Assay for Total Antioxidant Stores

Assay for cellular antioxidant stores was performed with cell lines and with tissues that were harvested from nonirradiated or TBI Serpinb3a$^{-/-}$ and Serpinb3a$^{+/+}$ Balb/c background mice. Protein concentrations were standardized using a Bradford assay, and antioxidant reductive capacity and antioxidant status were measured using a commercial kit (Northwest Life Science Specialties LLC, Vancouver, WA). This assay measures the antioxidant

capacity of cells based on the ability of cellular antioxidants to reduce Cu^{++} to CU^{-}, which reacts with bathocuproine to form a colored complex with absorbance at 480–490 nm. The antioxidant activity was compared to a standard curve generated using Trolox units (milliequivalents) and all data were expressed in Trolox units (13).

Apotag Assay for Apoptosis in Individual Cells

Serpinb3a$^{-/-}$ and Serpinb3a$^{+/+}$ Balb/c background strain bone marrow stromal cells were irradiated to 10 Gy and stained at various times postirradiation, including 24 h, using an *In Situ* Cell Death Kit Detection Kit, TMR red (Roche Diagnostics, Basel, Switzerland) according to manufacturer directions (13).

Statistical Analysis

In vivo radiation survival curves, performed in duplicate, are reported sequentially. Statistical analyses were performed using single-hit, multi-target or linear-quadratic models, n = 3 for each arm (10). Significant findings were by *P* value calculations using a Student's *t* test. Comparing Serpinb3a$^{-/-}$ with Serpinb3a$^{+/+}$ Balb/c background LTBMCs: data for the numbers of cobblestone islands, (primitive hematopoietic – stem cell containing flattened colonies on the adherent layer) (10), nonadherent cell numbers, percentage of confluence of adherent cells, days 7 and 14 colony counts were collected at weeks 1–20. At each week, the number of cobblestone islands for each mouse culture were counted from four cultures, then calculated by averaging the numbers. At each week, the Serapinb3a$^{-/-}$ group was compared to Balb/c group using the two-sided two-sample *t* test on the averaged numbers. Since this was an exploratory study, *P* values were not adjusted for multiple comparisons. Similar calculations and tests were performed for the nonadherent cell numbers and percentage of confluence of adherent cells. Days 7 and 14 colony count data were compared between Serapinb3a$^{-/-}$ and Serpinb3a$^{+/+}$ Balb/c background groups at each week using the two-sided two-sample *t* test.

The *in vitro* radiation survival curves were analyzed using both the linear-quadratic model and the single-hit multi-target model, and were compared using D_0 (final slope representing multiple-event killing) and ñ (extrapolation number measuring width of the shoulder on the radiation survival curve) (10, 13). Results for D_0 and ñ were shown as the mean ± SEM from multiple measurements and compared using the two-sided two-sample *t* test. For the other continuous end points, comparisons were also performed using a *t* test if they were normally distributed, or, otherwise, using a Wilcoxon rank-sum test.

Data for gene expression were summarized as mean ± standard deviation for each group. For each of multiple gene transcripts, each comparison was performed using the two-sided two-sample *t* test. $P < 0.05$ was considered significant. Since this was an exploratory study, *P* values were not adjusted for multiple comparisons. Western blot analysis for proteins was quantitated by densitometry as published elsewhere (9).

RESULTS

Radioresistance of Serpinb3a$^{-/-}$ Mice

Total-body irradiation was delivered to Serpinb3a$^{-/-}$ male and female compared to control Serpinb3a$^{+/+}$ Balb/c male and female mice. In two separate experiments, Serpinb3a$^{-/-}$ mice were significantly radioresistant after receiving 8.0 Gy TBI (Fig. 1). In two experiments, the 8 Gy dose was 100% lethal for Serpinb3a$^{+/+}$ Balb/c background mice before day 30 postirradiation. The observed shift over several months in percentage of animals displaying 30-day lethality after receiving the same TBI dose in different experiments with the same mice, same gender, genotype, age, weight and supplier has been reported elsewhere (24). Radiation dose rate, dosimetry, as measured in mouse phantoms, and dose homogeneity were performed using mouse phantoms produced by Dr. Ke Sheng, UCLA Center for Medical Countermeasures against Radiation (CMCR) Consortium, and were tested and found to be with the margin error provided by the CMCR/NIAID “dose harmonization” standards in a previously published work (9). The irradiation conditions are described in Materials and Methods. The 100% lethality of 8 Gy TBI to Serpinb3a$^{+/+}$ Balb/c background mice was adjusted for by taking into consideration the genotype differences between Balb/c and the historical control C57BL/6 mouse strain, which is significantly more radioresistant, but which also shows a dose-drift of lethality ranging from 50% to 100% death at day 30 after 9.25 Gy TBI (24).

Histopathological evaluation of bone marrow, small intestine and colon from Serpinb3a$^{-/-}$ compared to Serpinb3a$^{+/+}$ Balb/c background mice demonstrated equivalent hypocellularity degrees in intestine and bone marrow tissues at day of death. The histological appearance was similar to that of TBI experiments published elsewhere (38). Thus, no differences in the pathology of early death in Serpinb3a$^{+/+}$ Balb/c background mice could be detected by histological criteria.

These results establish the radioresistance to TBI of Serpinb3a$^{-/-}$ mice compared to Serpinb3a$^{+/+}$ Balb/c background mice (Fig. 1). Serpinb3a$^{+/+}$ mice that received 8 Gy TBI all died by day 13 in one experiment (Fig. 1A), while 10% of Serpinb3a$^{-/-}$ Balb/c background mice survived to day 30 postirradiaiton. In a second experiment, 8 Gy TBI was also lethal for Serpinb3a$^{+/+}$ Balb/c background mice, while 30% of Serpinb3a$^{-/-}$ mice survived (Fig. 1B). There was no evidence of a different cause of death between genotypes with respect to seizures or change in behavior other than a more rapid onset of listlessness in the Serpinb3a $^{+/+}$ Balb/c mice.

Increased Longevity of Hematopoiesis in Serpinb3a$^{-/-}$ Mouse LTBMCs

A significant correlate to TBI resistance *in vivo* of a particular mouse strain has been shown to be an increased longevity of hematopoiesis in explanted bone marrow LTBMCs from those mice *in vitro* (10). This correlation has been attributed to an increased number of oxidative stress-resistant hematopoietic stem cells in the hematopoietic marrow microenvironment of each radioresistant strain (10). Hematopoietic stem cells in the marrow microenvironment of LTBMCs maintain contact with stromal cells, and establish a state of quiescence, preserving hematopoietic stem cell function for over 20 weeks *in vitro* (10). The

LTBMCs from the Serpinb3a$^{-/-}$ radioresistant strain generated hematopoietic progenitor cells forming colonies in secondary semi-solid media culture for longer duration compared to LTBMCs from marrow from radiosensitive mice (Fig. 2). There was also an increased duration of generation of both committed granulocyte macrophage progenitors (cells forming colonies of >50 cells detected at 7 days in semisolid media culture), as well as more primitive multilineage granulocyte/erythroid/megakaryocyte/macrophage progenitor cells forming >50 cell colonies at day 14 in semisolid media secondary culture (10). LTBMCs from Serpinb3a$^{-/-}$ mice demonstrated a significant increase in longevity of hematopoiesis, as evidenced by total cumulative production of nonadherent hematopoietic cells over 20 weeks in culture (Fig. 2, Supplementary Figs. S1–4 and Supplementary Tables S1–5; http://dx.doi.org/10.1667/RR15379.1.S1).

We next performed an analysis of the longevity of hematopoiesis measured as duration of production of days 7 and 14 colony-forming progenitors and total nonadherent hematopoietic cells. We also measured stability of the hematopoietic microenvironment in culture by quantitating confluence of cells forming the adherent layer and the persistence of large numbers of cobblestone islands, which are ≥ 50 cell-containing adherent clusters of primitive hematopoietic cells that are attached to the stromal cell layer. There was equivalent production between genotypes of colony-forming progenitors forming at days 7 and 14 of colony-forming cells (Supplementary Figs. S1–4 and Supplementary Tables S1–5 http://dx.doi.org/10.1667/RR15379.1.S1). However, there was an increased production of total nonadherent hematopoietic cells in Serpinb3a$^{-/-}$ mouse LTBMCs compared to Serpinb3a$^{+/+}$ Balb/c background marrow cultures (Fig. 2). The data indicate greater cell production by Serpinb3a$^{-/-}$ mouse marrow-derived cultures. Since this was an exploratory study, *P* values were not adjusted for multiple comparisons. Similar calculations and tests were performed for the nonadherent cell numbers and percentage of confluence of adherent cells. The days 7 and 14 colony count data were compared between Serapinb3a$^{-/-}$ and Serpinb3a$^{+/+}$ Balb/c background groups at each week using the two-sided two-sample *t* test.

Radioresistance of Bone Marrow Hematopoietic Progenitor Cells, IL-3-Dependent Cell Lines and Bone Marrow Stromal Cell Lines from Serpinb3a$^{-/-}$ Mice

We next quantitated radioresistance of freshly explanted marrow from each mouse genotype by clonogenic survival analysis. Freshly explanted bone marrow hematopoietic cells were compared to IL-3-dependent hematopoietic progenitor cell lines derived from each mouse genotype LTBMC. Bone marrow stromal cell lines were also tested for radioresistance in clonogenic survival analysis as described in Materials and Methods. It is not known how hematopoietic cells from LTBMCs generate permanent hematopoietic cell lines in IL-3 supplemented media, but they are known to be stable *in vitro* for decades and do not produce tumors *in vivo* (39) unless transformed to IL-3 independence by oncogene transfection (35, 36) or in rare instances by spontaneous malignant transformation. As shown in Fig. 3A, freshly removed bone marrow hematopoietic progenitor cells forming colonies in semisolid media showed significant radioresistance with Serpinb3a$^{-/-}$ compared to Serpinb3a$^{+/+}$ Balb/c fresh mouse marrow. IL-3-dependent hematopoietic progenitor cell lines derived from Serpinb3a$^{-/-}$ mouse marrow and bone marrow stromal cell lines were also radioresistant (Fig. 3B and C, respectively). The data establish the radioresistance of

different cell phenotypes (hematopoietic and mesenchymal) derived from the marrow of Serpinb3a$^{-/-}$ mice, and are consistent with the improved survival after TBI and relative radioresistance of mice to the hematopoietic syndrome.

Increased Antioxidant Stores in Irradiated Serpinb3a$^{-/-}$ Bone Marrow Stromal Cell Lines

We tested the antioxidant stores in Serpinb3a$^{-/-}$ compared to Balb/c bone marrow stromal cell lines *in vitro*. The increase in antioxidant stores in cell lines *in vitro* and organs *in vivo* by Trolox assay has been shown to correlate with resistance to oxidative stress including irradiation (13, 37). As shown in Fig. 4, total antioxidant stores were increased at baseline in Serpinb3a$^{-/-}$ compared to Serpinb3a$^{+/+}$ Balb/c bone marrow stromal cell lines, and antioxidant store levels remained elevated in Serpinb3a$^{-/-}$ stromal cell lines after 5 Gy or 10 Gy irradiation. These two radiation doses have been used previously for this assay (11, 13).

Different Levels of RNA Transcripts and Proteins Associated with the Stress and Inflammation Response in Irradiated Serpinb3a$^{-/-}$ Cell Lines and in Mice

We tested the effect of radiation induction of RNA and protein levels for inflammatory cytokine and stress response transcripts and proteins, respectively, in 10 Gy irradiated bone marrow stromal cell lines *in vitro*. In addition, mice received 8.0 Gy TBI, and tissue was then explanted for RNA transcript analysis and plasma protein level measurement. The data revealed significant differences in radiation-induced levels of RNA transcripts for several relevant biomarkers of radioresistance in Serpinb3a$^{-/-}$ marrow stromal cell lines (Fig. 5). Levels of RNA transcripts increased in Serpinb3a$^{-/-}$ stromal cells for MnSOD and p21, which are consistent with radioresistance (Fig. 5). There was also a decrease in the levels of RNA transcripts for p53 and TGF-β in Serpinb3a$^{-/-}$ bone marrow stromal cell lines compared to those from Serpinb3a$^{+/+}$ Balb/c background strain marrow, also consistent with radioresistance. The data support the conclusion that Serpinb3a$^{-/-}$ mice and cell lines have a reduced inflammatory response to radiation associated with increased antioxidant capacity, and reduced levels of RNA for radiation-induced biomarkers of inflammation (Fig. 5) (The differences between mouse genotypes in other transcript levels are shown in Supplementary Fig. S5; http://dx.doi.org/10.1667/RR15379.1.S1).

We next quantitated the levels of radiation-induced stress and inflammation-related proteins (9) in the plasma of 8.0 Gy TBI mice, and in 10 Gy irradiated bone marrow stromal cell lines. The plasma data revealed a reduced level of radiation-induced exotaxin, G-CSF, IL-6, and MCP-1 proteins over 5 days after TBI with Serpinb3a$^{-/-}$ mice (Fig. 6). Data on multiple other plasma proteins and with irradiated marrow stromal cell lines are shown in Supplementary Fig. S6A and B (http://dx.doi.org/10.1667/RR15379.1.S1), respectively. The data are consistent with a reduced radiation-induced stress and inflammation response in Serpinb3a$^{-/-}$ mice and cell lines.

The increased postirradiation levels of MnSOD, RNA (Fig. 5) and decreased levels of inflammatory response proteins (Fig. 6) in Serpinb3a$^{-/-}$ mouse plasma and in irradiated stromal cell lines (Supplementary Fig. S6B; http://dx.doi.org/10.1667/RR15379.1.S1) were confirmed for MnSOD (SOD2) protein levels by Western blot (Fig. 7). We did not measure the p53, p21 and TGF-β protein levels by Western blot, since the Western blot for MnSOD

was performed to validate the Luminex assay, not to confirm the results with the Luminex assay as was done in studies reported elsewhere (9). JNK-phosphorylation, a marker of radiation-induced apoptosis, was significantly reduced at 24 h in irradiated Serpinb3a$^{-/-}$ cell lines compared to Serpinb3a$^{+/+}$ Balb/c cells (Fig. 7). The data show a decreased, overall, radiation-induced stress response in Serpinb3a$^{-/-}$ cells and also suggested that there would be less apoptosis. The increased levels of antioxidant stores detected with Serpinb3a$^{-/-}$ mouse cell lines (Fig. 4) are also consistent with radioresistance and also suggested that there would be less apoptosis. We next measured the levels of the radiation-induced apoptosis-associated phosphorylated protein p-JNK by Western blot. There was a baseline decrease and less radiation induction of p-JNK in Serpinb3a$^{-/-}$ cells *in vitro* (Fig. 7). The signaling pathways incorporating Serpinb3a include that related to JNK and present a possible mechanism for the decreased levels of p-JNK in Serpinb3a$^{-/-}$ mice. We next sought to determine whether the decreased p-JNK was related to decreased apoptosis after irradiation, as a possible mechanism for the radioresistance in Serpinb3a$^{-/-}$ mice and derived cell lines.

Decreased Apoptosis in Irradiated Serpinb3a$^{-/-}$ Bone Marrow Stromal Cell Lines

The above data were consistent with a role of Serpinb3a in decreasing the apoptosis pathway of mouse bone marrow after irradiation. To determine whether the absence of Serpinb3a was associated with decreased apoptosis, we carried out apotag assay to quantitate irradiation induced apoptosis in irradiated Serpinb3a$^{-/-}$ compared to Serpinb3a$^{+/+}$ Balb/c mouse bone marrow stromal cell lines. These cell lines were used as a measurement of *in vivo* responses of tissues. As shown in Fig. 8, there was a decrease in radiation-induced apoptosis with irradiated Serpinb3a$^{-/-}$ mouse marrow stromal cell lines. These results with reduced apoptosis are consistent with the increased levels of MnSOD and reduced JNK-P in irradiated Serpinb3a$^{-/-}$ cells. Furthermore, the results showing decreased radiation-induced apoptosis are consistent with increased antioxidant stores in Serpinb3a$^{-/-}$ cells and, specifically, the increased MnSOD protein levels measured by Western blot in irradiated Serpinb3a$^{-/-}$ cells.

Lack of Further Radioprotection of Serpinb3a$^{-/-}$ Stromal Cell Lines by Radiation Mitigators, JP4–039 or Necrostatin-1

Radiation-induced cell death pathways include apoptosis and necroptosis (9) and specific drugs are known to block each pathway (9). We tested whether clonal Serpinb3a$^{-/-}$ and Serpinb3a$^{+/+}$ Balb/c marrow stromal cells were susceptible to radiation-induced cell death by these pathways. The effect of the anti-apoptotic drug (JP4–039) (9) and anti-necroptotic drug (necrostatin-1) (9) was next tested. The results showed no detectable effect of either drug on the radiation clonogenic survival of Serpinb3a$^{-/-}$ cells. In contrast, there was significant radioresistance induced by each drug with Serpinb3a$^{+/+}$ Balb/c cells (Fig.9). The shoulder on the survival curve was significantly increased in Serpinb3a$^{+/+}$ Balb/c cultures treated with JP4–039 or necrostatin-1 compared to the control levels in Serpinb3a$^{+/+}$ Balb/c bone marrow stromal cells. JP4–039 and necrostatin-1 treated irradiated Serpinb3a$^{+/+}$ Balb/c bone marrow stromal cell cultures showed an ñ of 15.± 61.5 or 11.5 ± 1.4, respectively, compared to 7.4 ± 0.7 for control Serpinb3a$^{+/+}$ Balb/c bone marrow stromal cells (P = 0.0022 or 0.0239, respectively). These data reveal that Serpinb3a$^{-/-}$ cells were not

detectably further radioprotected by either a drug that blocks apoptosis or a drug that blocks necroptosis. The results suggest that Serpinb3a$^{-/-}$ marrow stromal cells were intrinsically radioresistant by a mechanism that neutralized or obviated induction of further radioresistance by drugs known to inhibit apoptosis and necroptosis.

DISCUSSION

The current results demonstrate that Serpinb3a$^{-/-}$ mice are resistant to TBI compared to Serpinb3a$^{+/+}$ Balb/c control mice. The dose rate used, 320 cGy/min, was shown to be unrelated to survival at lower dose rate, using the cesium irradiator (9). In multiple experiments in other mouse strains, the consistent TBI dose has been shown to produce a shift in lethality between experiments based on biologic differences in groups of mice from the same supplier (24). Both hematopoietic and mesenchymal stem cells (stromal cells) of Serpinb3a$^{-/-}$ mouse bone marrow were radioresistant. Radioresistance correlated to increased longevity of hematopoiesis in Serpinb3a$^{-/-}$ LTBMCs and increased levels of antioxidants including MnSOD in derived cell lines. We used two radiation doses, 5 and 10 Gy, in studies of antioxidant stores based on prior studies (10, 11), which revealed these doses to be in either the linear portion of the clonogenic survival curve or 100% lethal, respectively. There were several radiation-induced increases in RNA transcripts including those associated with reduced apoptosis: MnSOD and p21 with Serpinb3a$^{-/-}$ cell lines, and these also showed decreased radiation-induced apoptosis by apotag staining *in vitro*.

Serpinb3a$^{-/-}$ mice and cell lines demonstrated increased cellular antioxidant stores, increased radiation-induced, and duration of expression of MnSOD, and decreased radiation-induced apoptosis. Molecular pathways linking Serpinb3a with JNK-phosphorylation, a component of the apoptosis pathway, suggest involvement of Serpinb3a in apoptosis (14–19).

One of the challenges in studying the role of SerpinB3 and B4 in normal tissues has been the few known human mutations. As a result, animal models such as mice are frequently used (4). In mice SerpinB3 and SerpinB4 are expanded into four genes, Serpinb3a, −b3b, −b3c, and −b3d, and three pseudogenes (1–3). Serpinb3a has been shown to inhibit cathepsin G, K, L, S, V, papain, Der p and human mast cell chymase. Serpinb3a inhibits cathepsin L and G. Serpinb3c and b3d have not been shown to have inhibitory functions (5–8). Because of this expanded inhibitory repertoire that encompasses many of the profiles of SerpinB3 and B4, the Serpinb3a$^{-/-}$ mice were established and selected for further study. Based on previously published studies, which suggested that SerpinB3/B4 would confer a pro-survival function to irradiated cell lines, we hypothesized that knockout of the SerpinB3/B4 ortholog (Serpinb3a in mice) would result in radiosensitivity compared to the background Balb/c strain. We observed the opposite result, namely, that Serpinb3a$^{-/-}$ mice and derived cell lines were in fact radioresistant. One possibility is that the absence of Serpinb3 during gestation of knockout mice may have upregulated other serpins or other pathways that increased antioxidant levels and induced radioresistance. The experiments to test this possible explanation are in progress.

The potential role of SerpinB3 and SerpinB4 in radioresistance of cancer cells compared to cells of normal tissue has not been fully elucidated. There is evidence that SerpinB3 is involved in radioresistance of some cancer cells (20–23). Squamous cell carcinoma and hepatocellular carcinoma specimens have been shown to overexpress SerpinB3 and such overexpression leads to resistance to apoptosis, while suppression leads to an increased susceptibility to apoptosis (23). SRP-6 in *C. elegans* has a similar inhibitory profile to SerpinB3 and B4 in humans (6).

SerpinB3 and SerpinB4 were isolated from squamous cell carcinoma of the uterine cervix. Originally, named tumor antigen-4 (TA-4) and subsequently changed to squamous cell carcinoma antigen (SCCA), later studies showed that the antigen was composed of a mixture of two isoforms that are 98% and 92% identical at the nucleotide and amino acid sequences, respectively (7). Kinetics analysis revealed that Serpinb3 inhibits papain and the papain-like cysteine proteases cathepsin K, L, and S (8). SerpinB4 inhibits chymotrypsin-like serine proteases including chymase, cathepsin G, and Der p. Another study showed that SerpinB3 enhanced endoplasmic reticulum stress-induced cell apoptosis by causing subsequent cleavage and activation of caspase-8, while inhibiting necrosis-induced by lysosomal injury (6, 7). A human renal epithelial cell line was transfected to express SerpinB3 and B4, and the cells were then resistant to radiation-induced apoptosis compared to the non-transfected control cell lines. The transfected cells had suppressed activity levels of caspase 3 and 9, which decreased apoptosis and the expression of SerpinB3-and B4-suppressed signaling by p38 MAPK, a proapoptotic molecule. There was reduced phosphorylation of p38 MAPK and MKK3/MKK6 (7). The data with human cancer cell lines are opposite to our results with normal tissue in Serpinb3a$^{-/-}$ mice and derived cell lines.

Multiple death pathways are involved in radiation killing of cell lines in culture and mouse tissues *in vivo* including: apoptosis (24, 25), necroptosis (9, 26) and ferroptosis (27). Serpinb3a$^{-/-}$ cells showed decreased radiation-induced apoptosis (Fig. 8), which may be mediated by a robust upregulation of the transcripts for anti-apoptotic proteins including MnSOD (12), p21 (28, 29) and NF-κβ (9), and a marked downregulation of the transcripts for pro-apoptotic proteins including p53, AP-1, Gadd45 and TGF-β (Fig. 5 and Supplementary Fig. S5; http://dx.doi.org/10.1667/RR15379.1.S1). MnSOD protects cells against radiation-induced apoptosis by eliminating mitochondrial reactive oxygen species (ROS) and stabilizing the mitochondrial membrane (30, 31). p21 is known to inhibit apoptosis in response to DNA stress (28). NF-κβ governs the expression of a variety of genes (including MnSOD and p21) and its overall pro- or anti-apoptotic role is determined by the apoptotic stimulus (9). In response to radiation, NF-κβ target genes mediate a number of survival pathways that lead to adaptive radioresistance.

Accumulating evidence suggests that MnSOD is a key NF-κβ effector gene in radioresistance (32). In addition, NF-κβ inhibits JNK-mediated pro-apoptosis. Our data in Fig. 7 confirm the increased MnSOD expression and reduced JNK activation in Serpinb3a$^{-/-}$ cells, suggesting that NF-κβ may be a key mediator of Serpinb3a knockdown-induced radioresistance. Activated JNK translocates to mitochondria and phosphorylate BH3-only family of proteins to suppress the anti-apoptotic activity of Bcl2 or Bcl-XL. JNK also stimulates the release of cytochrome c via a Bid-Bax-dependent mechanism (33). In

addition, JNK activates AP-1, which in turn, leads to the expression of proapoptotic genes including p53. Gadd45 is a target gene of p53, which acts as an initiator of JNK/p38 signaling. TGF-β induces expression of Gadd45 via SMAD signaling and promotes apoptosis. Thus, pro-apoptotic factors JNK, Ap-1, p53 and Gadd45 form a positive feedback loop that amplifies the apoptotic signaling to commit cell death.

The significant downregulation of several proteins in Serpinb3a$^{-/-}$ cells may relate to the decreased radiation-induced apoptosis and explain their radioresistance. The detailed mechanism of how the absence of Serpinb3a regulates the pro- and anti-apoptotic factors is not clear. Interacting partners of SerpinB3/B4 that might regulate apoptosis include: RASSF7, which negatively regulates JNK signaling by inhibiting MKK7; and Rbm24, which prevents eIF4E from binding to p53 mRNA, and then inhibits p53 translation. Whether Serpinb3a inhibits RASSF7 and Rbm24 to explain the reduced JNK activation and p53 expression in Serpinb3a$^{-/-}$ cells is the subject of further studies. A potential signaling network that mediates the radioresistance of Serpinb3a$^{-/-}$ cells is shown in Fig. 10A. A summary of all data is shown in Fig. 10B.

We observed that protein responses to radiation in Serpinb3a$^{-/-}$ cell lines and mouse plasma were generally blunted compared to levels in control Serpinb3a$^{+/+}$ Balb/c background mice. It has been reported that Serpinb3a$^{-/-}$ mice display attenuated pro-inflammatory responses (34) and expression of SerpinB3/B4 is elevated in human inflammatory diseases (1–3, 7). As shown in Supplementary Fig. S6 (http://dx.doi.org/10.1667/RR15379.1.S1), pro-inflammatory cytokines including IL-1β and IL-17, and chemokines including IP-10 and MIG, were significantly upregulated in the stromal cells of Serpinb3a$^{+/+}$ Balb/c mice in response to radiation, while in Serpinb3a$^{-/-}$ mice, levels did not change (e.g., IP-10) or were significantly downregulated (e.g., MIG). Our previously published study (9) suggests that pro-inflammatory cytokines and chemokines, including IP-10 and MIG, may play a role in mediating excessive inflammatory responses to irradiation. These observations lead to the hypothesis that the blunted inflammatory responses induced by Serpinb3a knockdown could contribute to the radioresistance.

The failure to detect an effect of drugs that block apoptosis (JP4–039 (24, 25) or necroptosis (necrostatin-1 (9, 26) with Serpinb3a$^{-/-}$ marrow stromal cell lines suggests that the radioresistance of this cell line may be through mechanisms that overlap with both the apoptosis and necroptosis pathways. Further studies will be required to elucidate the molecular steps in radioresistance mediated by the absence of Serpinb3a and the precise mechanism of linkage of Serpinb3a deletion with reduced apoptosis.

Supplementary Material

Refer to Web version on PubMed Central for supplementary material.

ACKNOWLEDGMENTS

This work was supported by the National Institutes of Health (NIH grant no. U19-A1068021). This project used the UPCI Animal Facility, which is supported in part by a National Cancer Institute Cancer Center Support Grant (no. P30CA047904).

REFERENCES

1. Heit C, Jackson BC, McAndrews M, Wright MW, Thompson DC, Silverman GA, et al. Update of the human and mouse SERPIN gene superfamily. Hum Genomics 2013; 7:22. [PubMed: 24172014]
2. Gatto M, Iaccarino L, Ghirardello A, Bassi N, Pontisso P, Punzi L, et al. Serpins, immunity and autoimmunity: old molecules, new functions. Clin Rev Allergy Immunol 2013; 45:267–80. [PubMed: 23325331]
3. Law RH, Zhang Q, McGowan S, Buckle AM, Silverman GA, Wong W, et al. An overview of the serpin superfamily. Genome Biol 2006; 7:216. [PubMed: 16737556]
4. Silverman GA, Whisstock JC, Bottomley SP, Huntington JA, Kaiserman D, Luke CJ, et al. Serpins flex their muscle: I. putting the clamps on proteolysis in diverse biological systems. J Biol Chem 2010; 285:24299–305. [PubMed: 20498369]
5. Silverman GA, Whisstock JC, Askew DJ, Pak SC, Luke CJ, Cataltepe S, et al. Human clade B serpins (ov-serpins) belong to a cohort of evolutionarily dispersed intracellular proteinase inhibitor clades that protect cells from promiscuous proteolysis. Cell Mol Life Sci 2004; 61:301–25. [PubMed: 14770295]
6. Luke CJ, Pak SC, Askew YS, Naviglia TL, Askew DJ, Nobar SM, et al. An intracellular serpin regulates necrosis by inhibiting the induction and sequelae of lysosomal injury. Cell 2007; 130:1108–19. [PubMed: 17889653]
7. Sun Y, Sheshadri N, Zong WX. SERPINB3 and B4: from biochemistry to biology. Semin Cell Dev Biol 2017; 62:170–7. [PubMed: 27637160]
8. Askew DJ, Askew YS, Kato Y, Turner RF, Dewar K, Lehoczky J, et al. Comparative genomic analysis of the clade B serpin cluster at human chromosome 18q21: amplification within the mouse squamous cell carcinoma antigen gene locus. Genomics 2004; 84:176–84. [PubMed: 15203215]
9. Steinman J, Epperly M, Hou W, Willis J, Wang H, Fisher R, et al. Improved total-body irradiation survival by delivery of two radiation mitigators that target distinct cell death pathways. Radiat Res 2018; 189:68–83. [PubMed: 29140165]
10. Berhane H, Epperly MW, Goff J, Kalash R, Cao S, Franicola D, et al. Radiologic differences between bone marrow stromal and hematopoietic progenitor cell lines from Fanconi anemia (Fancd2–/–) mice. Radiat Res 2014; 181:76–89. [PubMed: 24397476]
11. Sivananthan A, Shields D, Fisher R, Hou W, Zhang X, Franicola D, et al. Continuous one year oral administration of the radiation mitigator, MMS350, after total-body irradiation, restores bone marrow stromal cell proliferative capacity and reduces senescence in Fanconi anemia (Fanca–/–) mice. Radiat Res 2019; 191:139–53. [PubMed: 30499383]
12. Rajagopalan MS, Stone B, Rwigema JC, Salimi U, Epperly MW, Goff J, et al. Intraesophageal manganese superoxide dismutaseplasmid liposomes ameliorate novel total-body and thoracic radiation sensitivity of NOS1–/– mice. Radiat Res 2010; 174:297–312. [PubMed: 20726721]
13. Shinde A, Berhane H, Rhieu BH, Kalash R, Xu K, Goff J, et al. Intraoral mitochondrial-targeted GS-nitroxide, JP4–039, radio-protects normal tissue in tumor-bearing radiosensitive Fancd2–/– (C57BL/6) mice. Radiat Res 2016; 185:134–50. [PubMed: 26789701]
14. Turato C, Calabrese F, Biasiolo A, Quarta S, Ruvoletta M, Tono N, et al. SERPINB3 modulates TGF-beta expression in chronic liver disease. Lab Invest 2010; 90:1016–23. [PubMed: 20212457]
15. Ciscata F, Sciacovelli M, Villano G, Turato C, Bernardi P, Rasola A, et al. SERPINB3 protects from oxidative damage by chemotherapeutics through inhibition of mitochondrial respiratory complex I. Oncotarget 2014; 5:2418–27. [PubMed: 24810714]
16. Baldwin AS Jr. The NF-kappa B and I kappa B proteins: new discoveries and insights. Annu Rev Immunol 1996; 14:649–83. [PubMed: 8717528]
17. Lawrence T The nuclear factor NF-kappaB pathway in inflammation. Cold Spring Harb Perspect Biol 2009; 1:a001651. [PubMed: 20457564]
18. Vidalino L, Doria A, Quarta SM, Crescenzi M, Ruvoletto M, Frezzato F, et al. SERPINB3 expression on B-cell surface in autoimmune diseases and hepatitis C virus-related chronic liver infection. Exp Biol Med (Maywood) 2012; 237:793–802. [PubMed: 22829702]
19. Vidalino L, Doria A, Quarta S, Zen M, Gatta A, Pontisso P. SERPINB3, apoptosis and autoimmunity. Autoimmune Rev 2009; 9:108–12.

20. Uemura Y, Pak SC, Luke C, Cataltepe S, Tsu C, Schick C, et al. Circulating serpin tumor markers SCCA1 and SCCA2 are not actively secreted but reside in the cytosol of squamous carcinoma cells. Int J Cancer 2000; 89:368–77. [PubMed: 10956412]
21. Katagiri C, Nakanishi J, Kadoya K, Hibino T. Serpin squamous cell carcinoma antigen inhibits UV-induced apoptosis via suppression of c-JUN NH2-terminal kinase. J Cell Biol 2006; 172:983–90. [PubMed: 16549498]
22. Murakami A, Suminami Y, Hirakawa H, Nawata S, Numa F, Kato H. Squamous cell carcinoma antigen suppresses radiation-induced cell death. Br J Cancer 2001; 84:851–8. [PubMed: 11259103]
23. Ullman E, Pan J-A, Zong W-X. Squamous cell carcinoma antigen 1 promotes caspase-8-mediated apoptosis in response to endoplasmic reticulum stress while inhibiting necrosis induced by lysosomal injury. Mol Cell Biol 2011; 31:2902–19. [PubMed: 21576355]
24. Epperly MW, Wipf P, Fisher R, Franicola D, Beumer J, Li S, et al. Evaluation of different formulations and routes for the delivery of the ionizing radiation mitigator GS-nitroxide (JP4–039). In vivo 2018; 32:1009–23. [PubMed: 30150422]
25. Epperly MW, Sacher JR, Krainz T, Zhang X, Wipf P, Liang M, et al. Effectiveness of analogs of the GS-nitroxide, JP4–039, as total body irradiation mitigators. In vivo 2017; 31:39–43. [PubMed: 28064218]
26. Huang Z, Epperly M, Watkins SC, Greenberger JS, Kagan VE, Bayir H. Necrostatin-1 rescues mice from lethal irradiation. Biochim Biophys Acta 2016; 1862:850–6. [PubMed: 26802452]
27. Dar HH, Tyurina YY, Mikulska KA, Shrivastava I, Tyurin VA, Krieger J, et al. Pseudomonas aeruginosa utilizes host polyunsaturated phosphatidylethanolamines to trigger theft-ferroptosis in bronchial epithelium. J Clin Invest 2018; 128:4639–53. [PubMed: 30198910]
28. Gartel AL, Tyner AL. The role of the cyclin-dependent kinase inhibitor p21 in apoptosis. Mol Cancer Ther 2002; 1:639–49. [PubMed: 12479224]
29. Schick C, Pemberton PA, Shi G-P, Kamachi Y, Cataltepe S, Bartuski AJ, et al. Cross-class inhibition of the cysteine proteinases cathepsins K, L, and S by the serpin squamous cell carcinoma antigen 1: a kinetic analysis. Biochem 1998; 37:5258–66. [PubMed: 9548757]
30. Epperly MW, Travis EL, Sikora C, Greenberger JS. Magnesium superoxide dismutase (MnSOD) plasmid/liposome pulmonary radioprotective gene therapy: Modulation of irradiation-induced mRNA for IL-1, TNF-alpha, and TGF-beta correlates with delay of organizing alveolitis/fibrosis. Biol Blood Marrow Transplant 1999; 5:204–14. [PubMed: 10465100]
31. Epperly MW, Gretton JE, Bernarding M, Nie S, Rasul B, Greenberger JS. Mitochondrial localization of copper/zinc super-oxide dismutase (Cu/ZnSOD) confers radioprotective functions in vitro and in vivo. Radiat Res 2003; 160:568–78. [PubMed: 14565825]
32. Kalash R, Epperly MW, Goff J, Dixon T, Sprachman MM, Zhang X, et al. Amelioration of irradiation pulmonary fibrosis by a water-soluble bi-functional sulfoxide radiation mitigator (MMS350). Radiat Res 2013; 180:474–90. [PubMed: 24125487]
33. Dhanasekaran DN, Reddy EP. JNK signaling in apoptosis.Oncogene 2008; 27:6245–51. [PubMed: 18931691]
34. Sivaprasad U, Askew DJ, Ericksen MB, Gibson AM, Stier MT, Brandt EB, et al. A nonredundant role for mouse Serpinb3a in the induction of mucus production in asthma. J Allergy Clin Immunol 2011; 127:254–61. [PubMed: 21126757]
35. Zhang X, Fisher R, Shields D, Hou W, Franicola D, Epperly MW, et al. Malignant transformation of Fanconi anemia (FA) Fancd2–/– hematopoietic progenitor cells by single E6 or E7 oncogene of the human papillomavirus 16. In vivo 2019; 33:303–11. [PubMed: 30804107]
36. FitzGerald TJ, Santucci MA, Das IJ, Kase K, Pierce JH, Greenberger JS. The v-abl, c-fms, or v-myc oncogene induce radiation resistance of hematopoietic progenitor cell line 32D cl 3 at clinical low-dose-rate. Int J Radiat Oncol Biol Phys 1991; 21:1203–10. [PubMed: 1938518]
37. Epperly MW, Wegner R, Kanai AJ, Kagan V, Greenberger EE, Nie S, et al. Effects of MnSOD-Plasmid Liposome gene therapy on antioxidant levels in the irradiated murine oral cavity orthotopic tumors. Radiat Res 2007; 167:289–97. [PubMed: 17316075]

38. Goff JP, Epperly MW, Shields D, Wipf P, Dixon T, Greenberger JS. Radiobiologic effects of GS-nitroxide (JP4–039) in the hematopoietic syndrome. In vivo 2011; 25:315–24. [PubMed: 21576404]

39. Greenberger JS, Sakakeeny MA, Humphries KC, Eaves CG, Eckner RJ. Demonstration of permanent factor-dependent multipotential (erythroid/neutrophil/basophil) hematopoietic progenitor cell lines. Proc Natl Acad Sci U S A 1983; 80:2931–5. [PubMed: 6574462]

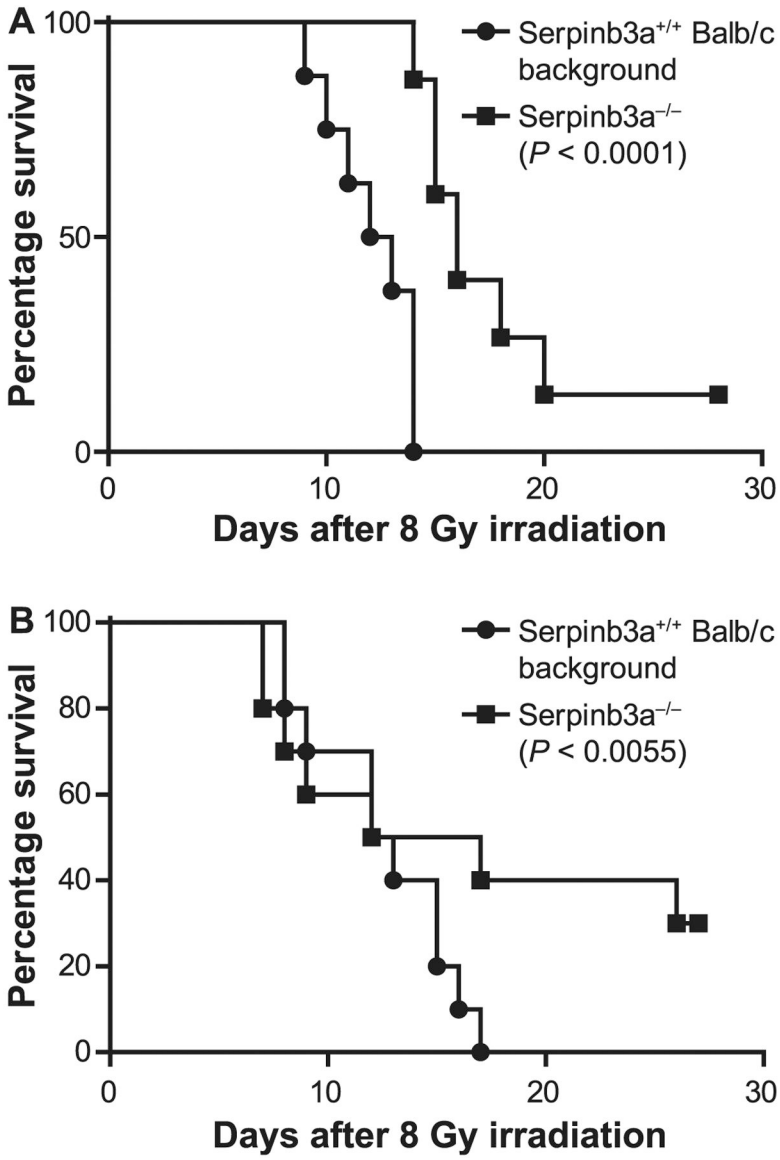

FIG. 1.

Serpinb3a$^{-/-}$ mice are radiation resistant. Panels A and B: Data presented for two separate experiments. Serpinb3a$^{-/-}$ and Serpinb3a$^{+/+}$ Balb/c background mice (n = 20) received 8 Gy TBI and were monitored for development of the hematopoietic syndrome, then sacrificed according to Institutional IACUC protocols. In two separate experiments ($P < 0.0001$ and $P = 0.0055$, respectively), Serpinb3a$^{-/-}$ mice were significantly radioresistant. Since this is an exploratory study, P values were not adjusted for multiple comparisons.

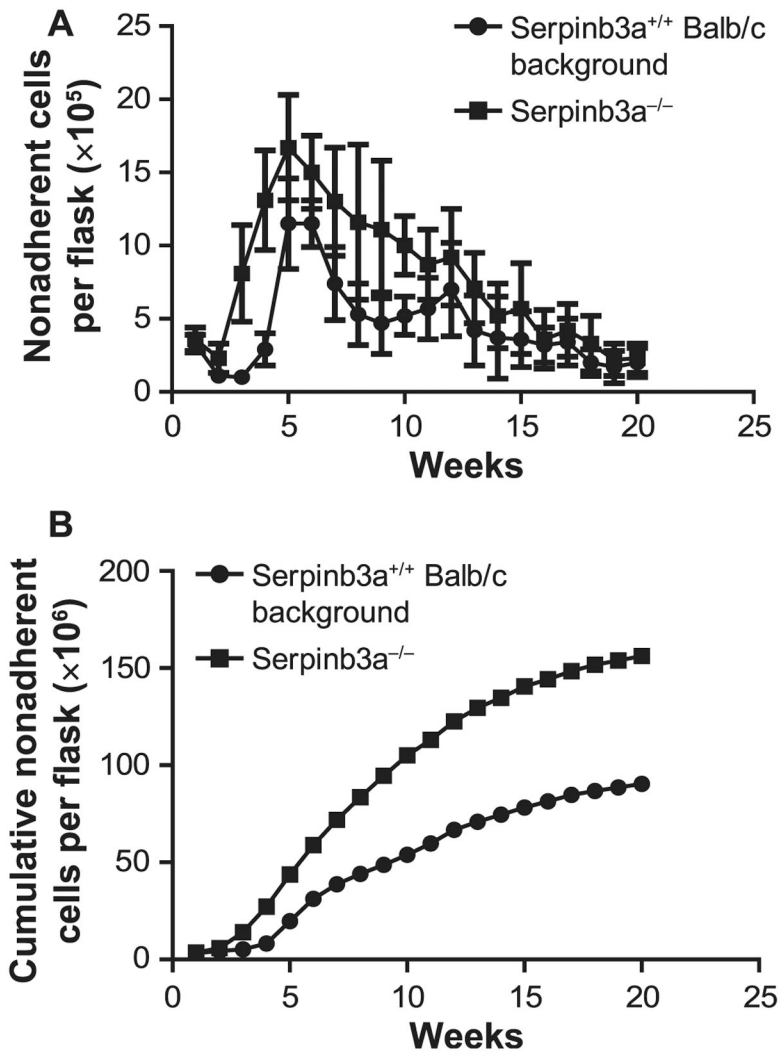

FIG. 2.

Serpinb3a$^{-/-}$ mouse long-term bone marrow cultures (LTBMCs) have increased duration of hematopoiesis compared to Serpinb3a$^{+/+}$ Balb/c background strain LTBMCs. Data are presented for total (panel A) and cumulative (panel B) nonadherent cells produced. There were 4 flasks (2 mice per genotype and 2 flasks/mouse consisting of marrow from one tibia and one femur per flask. The data include error bias from each flask, n = 4. For cumulative production (panel B) the results are pooled from the mean. Other parameters of hematopoiesis are shown in Supplementary Figs. S1–4 (http://dx.doi.org/10.1667/RR15379.1.S1). LTBMCs from Serpinb3a$^{-/-}$ and Serpinb3a$^{+/+}$ Balb/c mice were established and observed weekly for hematopoietic cell production and adherent cell layer confluence. Serpinb3a$^{-/-}$ LTBMCs demonstrated a significant increase in longevity of hematopoiesis, demonstrated by total cumulative production of hematopoietic cells over 20 weeks in culture. (n = 4 per genotype)

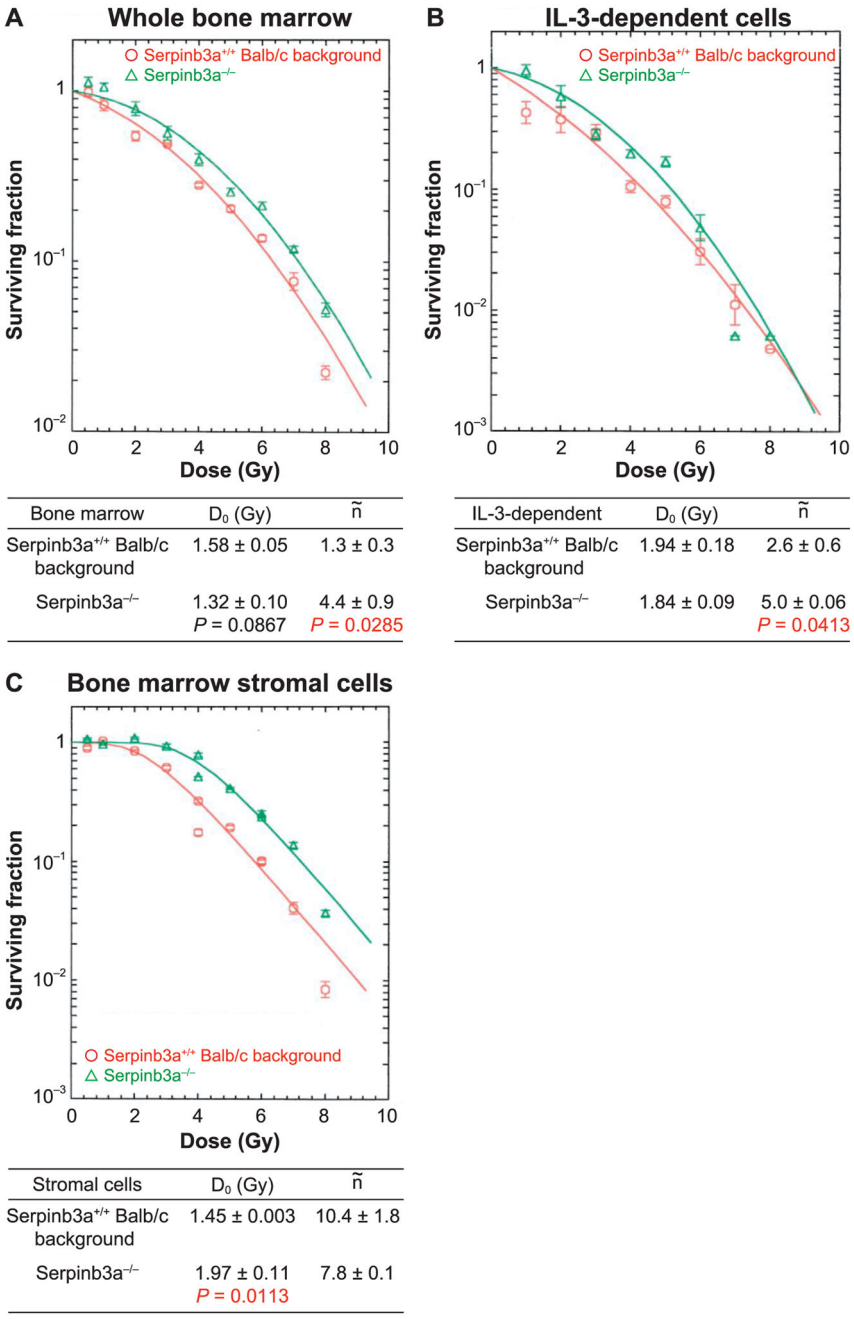

Bone marrow	D_0 (Gy)	$\tilde{n}$
Serpinb3a$^{+/+}$ Balb/c background	1.58 ± 0.05	1.3 ± 0.3
Serpinb3a$^{-/-}$	1.32 ± 0.10 *P* = 0.0867	4.4 ± 0.9 *P* = 0.0285

IL-3-dependent	D_0 (Gy)	$\tilde{n}$
Serpinb3a$^{+/+}$ Balb/c background	1.94 ± 0.18	2.6 ± 0.6
Serpinb3a$^{-/-}$	1.84 ± 0.09	5.0 ± 0.06 *P* = 0.0413

Stromal cells	D_0 (Gy)	$\tilde{n}$
Serpinb3a$^{+/+}$ Balb/c background	1.45 ± 0.003	10.4 ± 1.8
Serpinb3a$^{-/-}$	1.97 ± 0.11 *P* = 0.0113	7.8 ± 0.1

FIG. 3.

Bone marrow hematopoietic progenitor cells, IL-3-dependent cell lines, and bone marrow stromal cell lines from Serpinb3a$^{-/-}$ mice are radioresistant. Panel A: Bone marrow was isolated from Serpinb3a$^{-/-}$ and Serpinb3a$^{+/+}$ Balb/c mice, prepared into single cell suspensions, and analyzed using the clonogenic radiation survival as described in the Methods. Serpinb3a$^{-/-}$ bone marrow hematopoietic progenitor cells were radioresistant compared to Serpinb3a$^{+/+}$ Balb/c bone marrow, as demonstrated by an increased shoulder on the survival curve [n (extrapolation number (10)) = 4.4 ± 0.9 compared to 1.3 ± 0.3, *P* = 0.0285]. Panel B: Radiation survival curves were performed on IL-3-dependent cell lines

derived from Serpinb3a$^{-/-}$ and Serpinb3a$^{+/+}$ Balb/c mouse LTBMCs. The Serpinb3a$^{-/-}$ cell line was radioresistant compared to Serpinb3a$^{+/+}$ Balb/c cells, as demonstrated by an increased shoulder on the stromal line (n = 5.0 ± 0.06 compared to 2.6 ± 0.06, $P = 0.0413$). Panel C: The Serpinb3a$^{-/-}$ mouse bone marrow stromal cell line was radioresistant compared to Balb/c bone marrow stromal cells derived from LTBMCs, as shown by an increase in D_0 (1.97 ± 0.11 compared to 1.45 ± 0.003). The results are one of three separate experiments. (n = 3 per data point for this experiment).

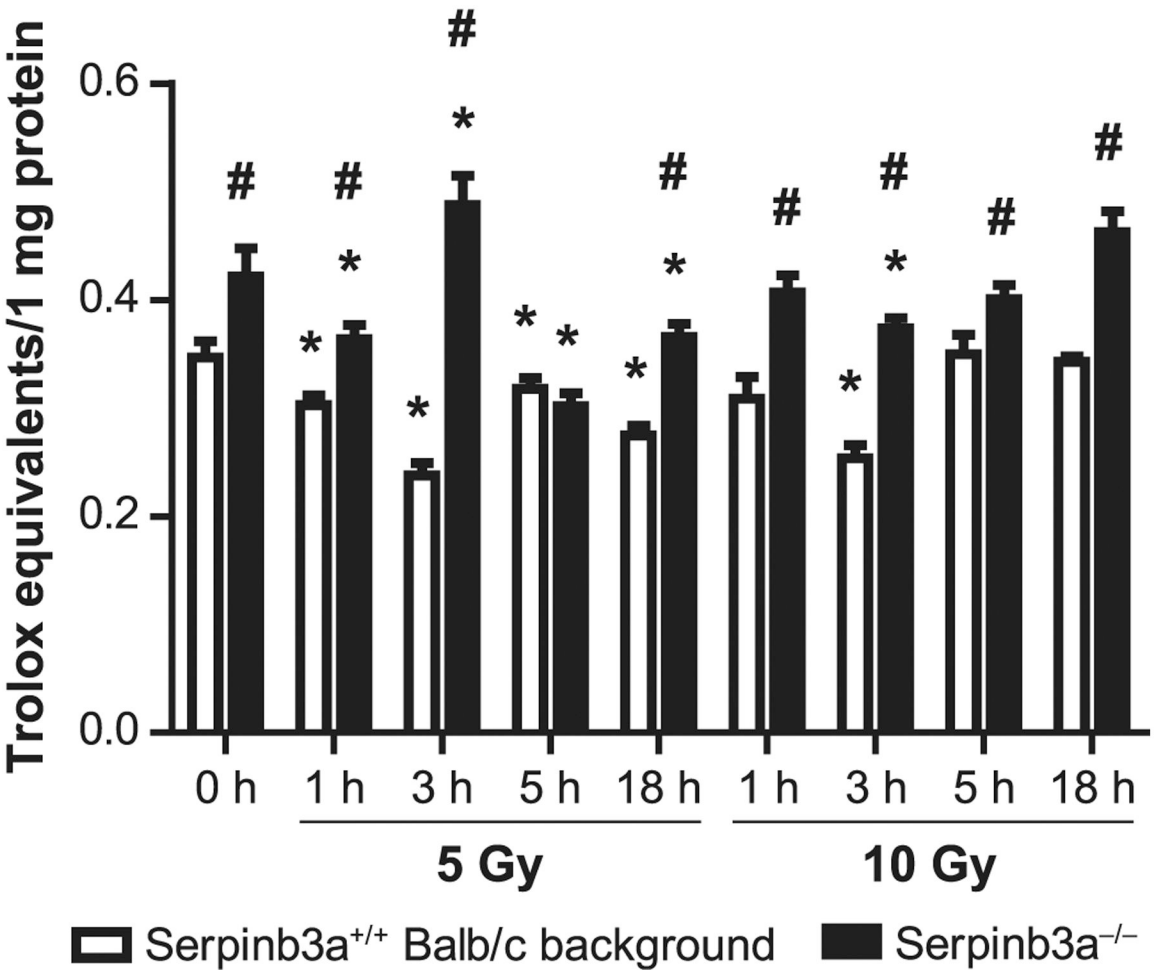

FIG. 4.

Serpinb3a$^{-/-}$ bone marrow stromal cells have increased antioxidant stores compared to Balb/c bone marrow stromal cells. Antioxidant stores were determined in Sepinb3a$^{-/-}$ and Serpinb3a$^{+/+}$ Balb/c bone marrow cells that received 5 or 10 Gy irradiation based on data with other bone marrow stromal cell lines in other experiments (10, 11), and reflecting a dose on the linear portion of the survival curve and a 100% lethal dose, respectively. Cells were harvested at 0, 1, 3, 5 and 18 h postirradiation. Antioxidant stores were measured in Serpinb3a$^{-/-}$ compared to Serpinb3a$^{+/+}$ Balb/c bone marrow stromal cell lines *in vitro*. Total antioxidant stores were increased at baseline in Serpinb3a$^{-/-}$ compared to Serpinb3a$^{+/+}$ Balb/c bone marrow stromal cell lines. Antioxidant store levels remained elevated in Serpinb3a$^{-/-}$ stromal cell lines after 5 or 10 Gy irradiation. (n = 3 per data point). *$P < 0.05$ compared to 0 h of respective strain; $^{\#}P < 0.05$ compared to Serpinb3a$^{+/+}$ Balb/c background at the same time.

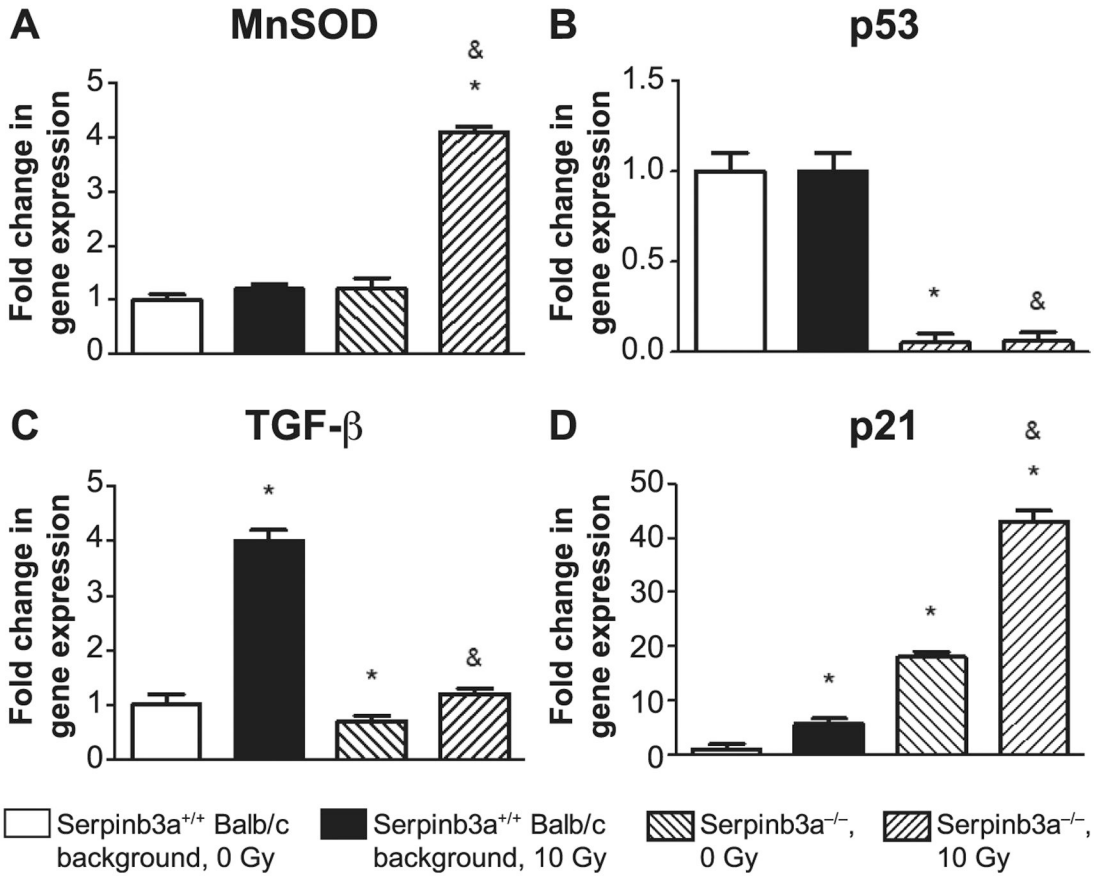

FIG. 5.

RT-PCR detection of radiation-induced genes from Serpinb3a$^{-/-}$ and Serpinb3a$^{+/+}$ Balb/c background strain bone marrow stromal cells. RNA was isolated from Serpinb3a$^{-/-}$ and Balb/c bone marrow stromal cells at 0 and 24 h after 10 Gy irradiation. Quantitative-PCR-RNA transcripts of stress response genes and inflammatory cytokines were performed with bone marrow stromal cell lines. RT-PCR in Serpinb3a$^{-/-}$ cells demonstrated increased radiation-induced mRNA for (panel A) MnSOD and (panel D) p21, and decreased expression of (panel B) p53 and (panel C) TGF-β. (Data with other radiation-induced RNA species are shown in Supplementary Fig. S5; http://dx.doi.org/10.1667/RR15379.1.S1). (n = 4 per data point). *$P < 0.05$ compared to Serpinb3a$^{+/+}$ Balb/c background, 0 Gy; $^{\#}P < 0.05$ compared to Serpinb3a$^{+/+}$ Balb/c background, 10 Gy. Results were standardized to Serpinb3a$^{+/+}$ Balb/c background.

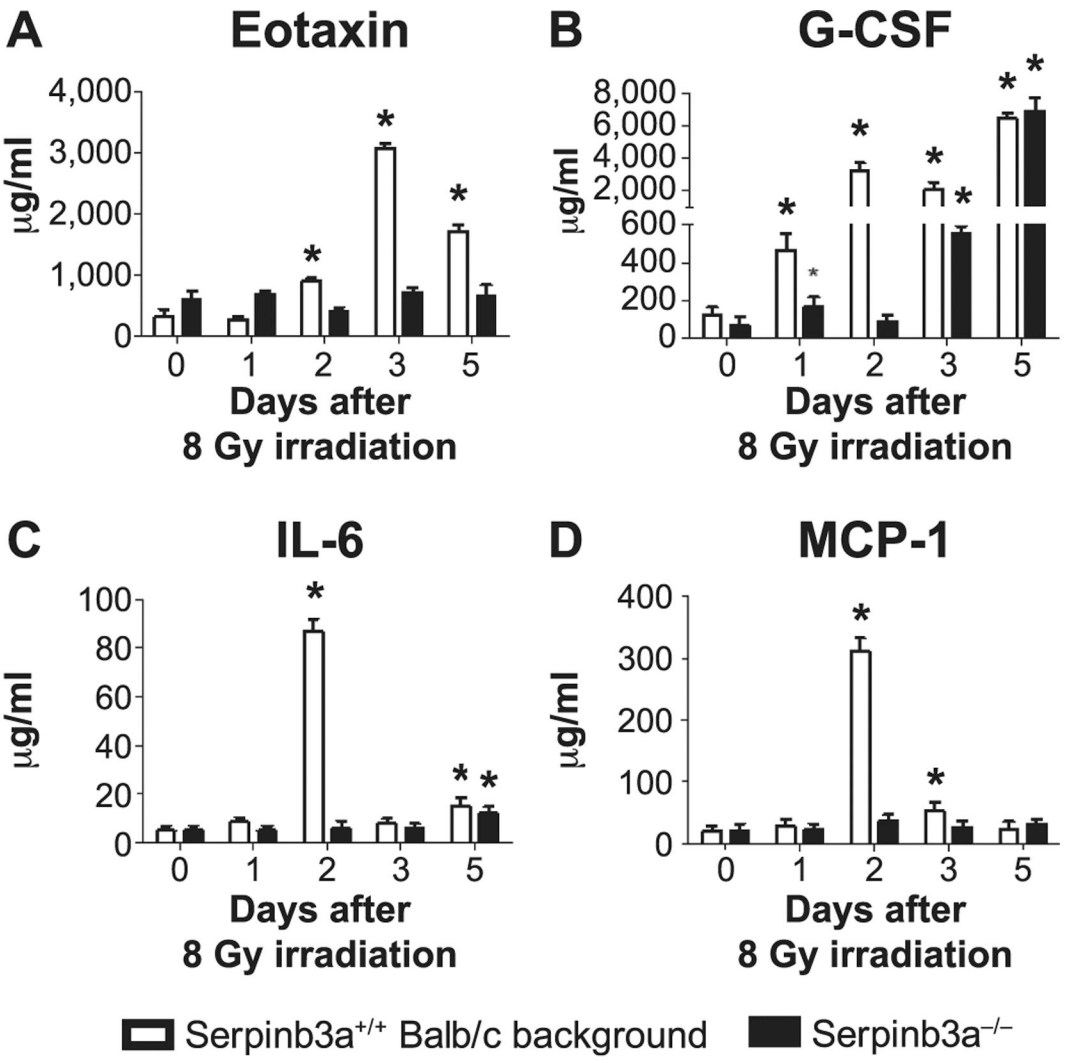

FIG. 6.

Different levels of proteins in irradiated Serpinb3a$^{-/-}$ compared to Serpinb3a$^{+/+}$ Balb/c background strain in mouse plasma over 5 days after 8.0 Gy TBI. Serpinb3a$^{-/-}$ and Serpinb3a$^{+/+}$ Balb/c mice were 8 Gy irradiated and plasma was harvested at days 1, 2, 3 or 5. Protein expression was determined using Luminex Assay as described in Materials and Methods. Significant differences were observed for many plasma proteins. Examples include (panels A–D): Eotaxin, G-CSF, IL-6 and MIP-1, respectively, all of which were suppressed in Serpinb3a$^{-/-}$ mice. Data for multiple other plasma patterns and cell line radiation-induced proteins are shown in Supplementary Figs. 6A and B, respectively (http://dx.doi.org/10.1667/RR15379.1.S1). *$P < 0.05$ for significantly increased expression compared to 0 Gy irradiation.

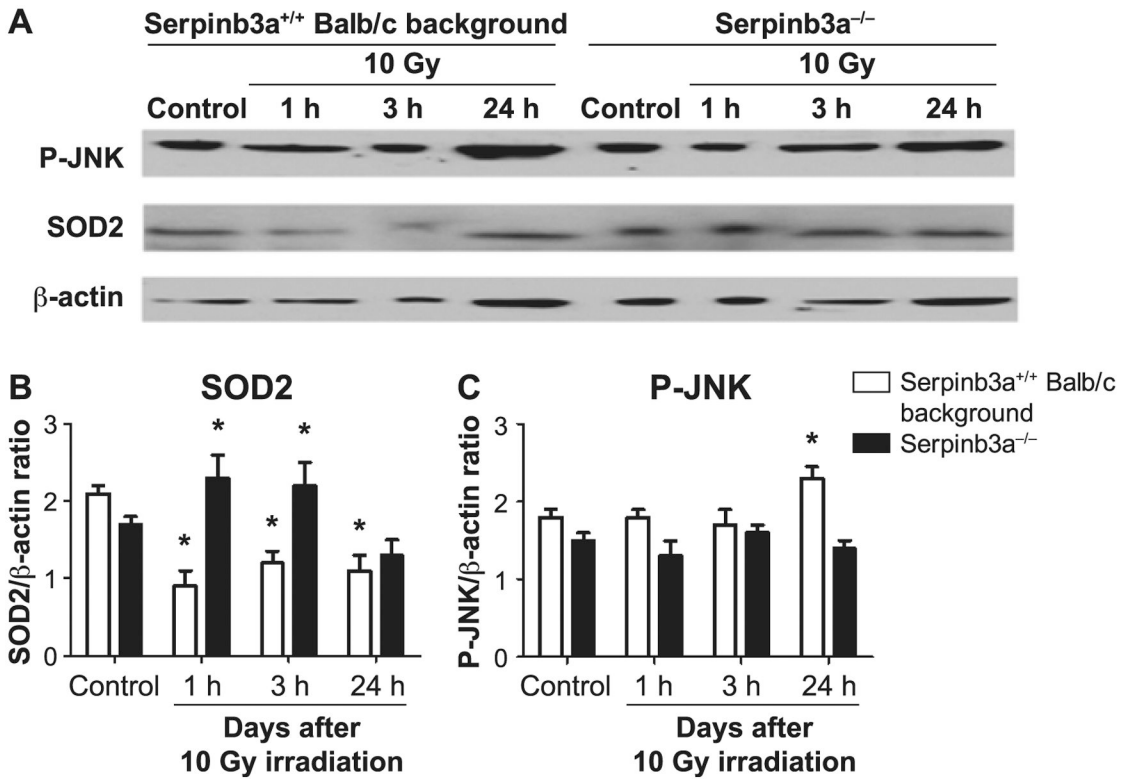

FIG. 7.

Western blot analysis of P-JNK and MnSOD (SOD2) protein after 10 Gy irradiation shows decreased radiation-induced P-JNK and increased MnSOD in Serpinb3a$^{-/-}$ compared to Serpinb3a$^{+/+}$ Balb/c mouse bone marrow stromal cells. At 0, 1, 3 and 24 h after 10 Gy irradiation of Serpinb3a$^{-/-}$ and Serpinb3a$^{+/+}$ Balb/c bone marrow stromal cells were collected, cells homogenized and Western blot analysis performed with antibodies to phosphorylated JNK and MnSOD. Panel A: After irradiation, Western blots showed increased P-JNK and decreased MnSOD levels in Serpinb3a$^{+/+}$ Balb/c bone marrow cells. Panels B and C: Bar graphs quantitating MnSOD and P-JNK levels from Fig. 7A. Quantitation of MnSOD (panel B) performed by comparisons with bactin expression demonstrated that Serpinb3a$^{-/-}$ bone marrow stromal cells had increased MnSOD expression compared to Serpinb3a$^{+/+}$ Balb/c bone marrow stromal cells. (*$P < 0.0001$ compared to control.) In contrast, as shown in panel C, JNK-phosphorylation, a marker of radiation-induced apoptosis, was significantly reduced in irradiated Serpinb3a$^{-/-}$ cell lines compared to Serpinb3a$^{+/+}$ Balb/c bone marrow stromal cells. (*$P = 0.0365$ compared to control.)

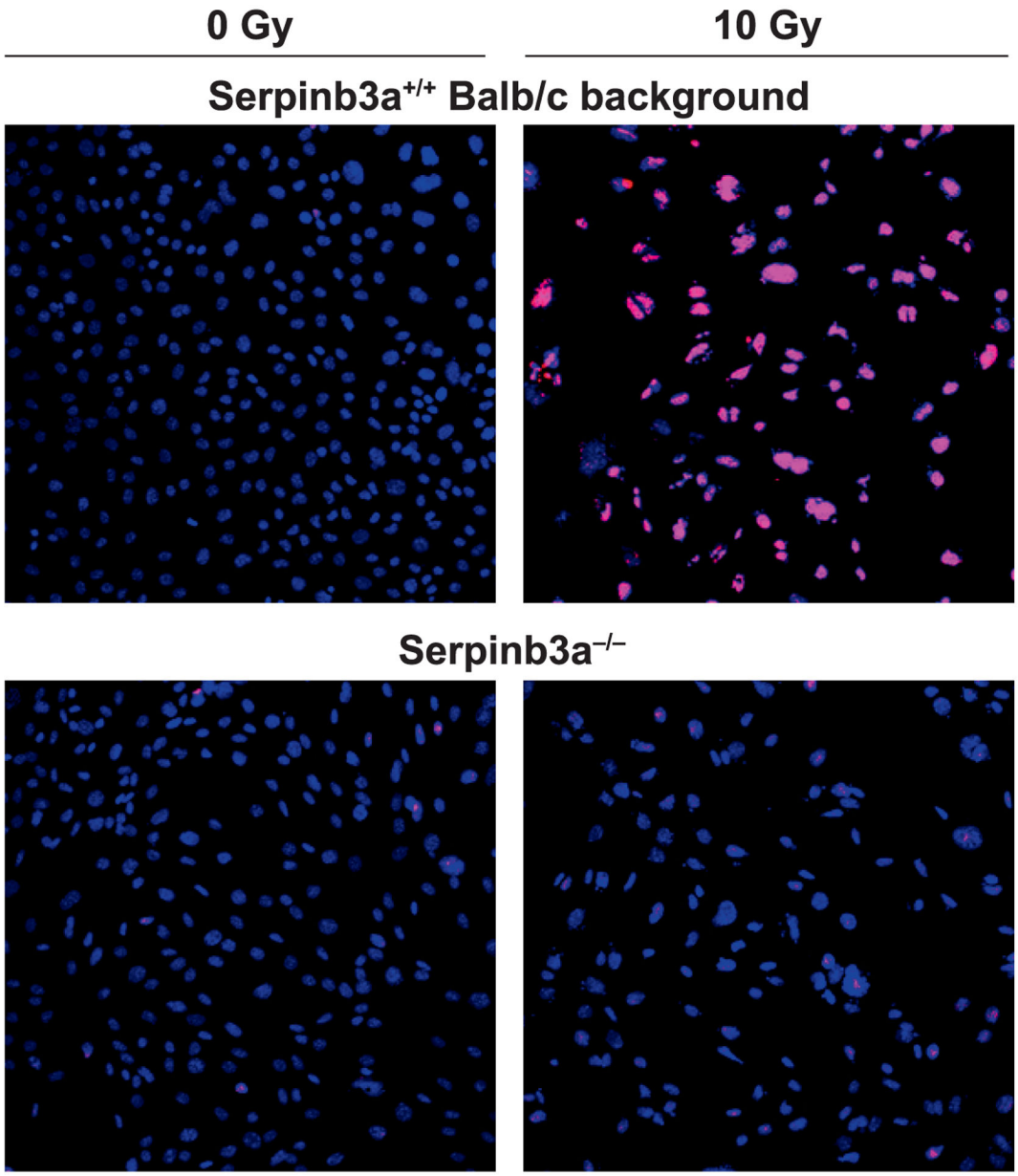

FIG. 8.

Reduced levels of radiation-induced apoptosis in Serpinb3a$^{-/-}$ compared to Serpinb3a$^{+/+}$ Balb/c bone marrow stromal cells. Serpinb3a$^{+/+}$ Balb/c and Serpinb3a$^{-/-}$ bone marrow stromal cells received 10 Gy irradiation and stained for apoptosis at 24 h. Ten slides of cell lines from mouse marrow stromal cell lines of each genotype were scored for percentage of 1,000 counted cells that were apotag positive. Serpinb3a$^{-/-}$ cells compared to Serpinb3a$^{+/+}$ Balb/c cell lines showed fewer apotag-positive cells. A representative figure shows Serpinb3a$^{-/-}$ cells compared to Serpinb3a$^{+/+}$ Balb/c cells. Serpinb3a$^{+/+}$ Balb/c cells had increased apoptosis, indicated by increased staining, as described in Materials and Methods (×100).

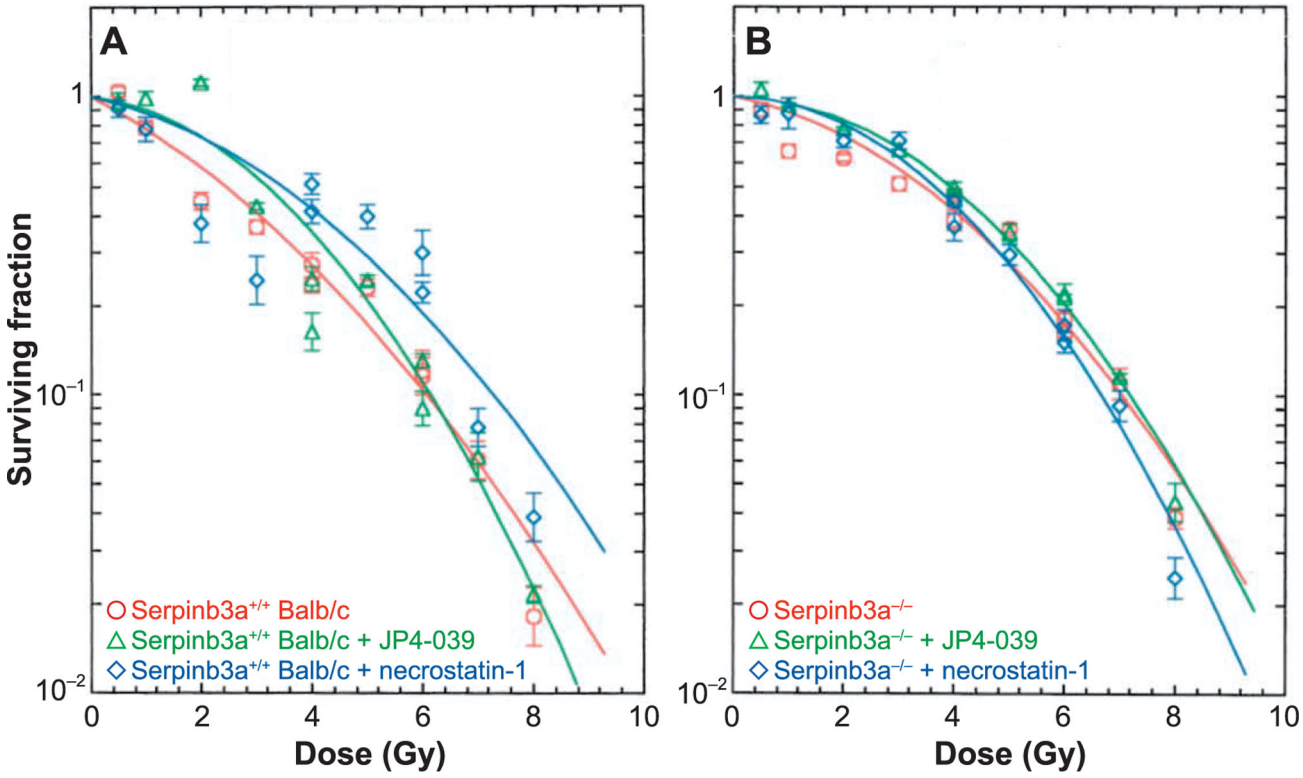

FIG. 9.

Lack of additional radioresistance in JP4–039 or necrostatin-1 treated Serpinb3a$^{-/-}$ marrow stromal cells. Serpinb3a$^{+/+}$ Balb/c (panel A) and Serpinb3a$^{-/-}$ (panel B) bone marrow stromal cell lines were treated with JP4–039 (10 mM) or necrostatin-1(10 m*M*) 1 h before irradiation, as described in the Materials and Methods, then plated for clonogenic survival curve assays, as described in the Materials and Methods.

A

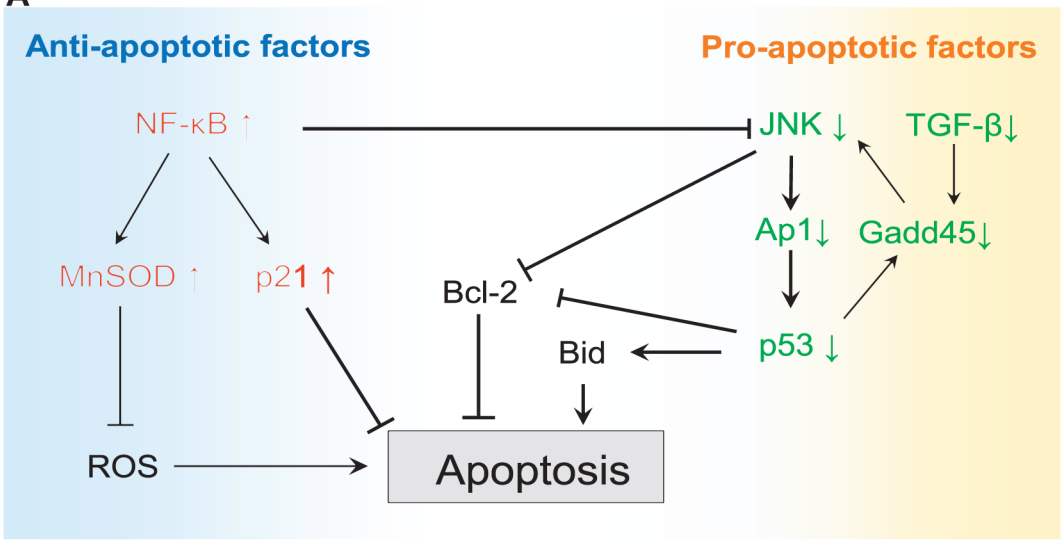

B

Assay	Result (Serpinb3a$^{-/-}$ relative to Serpinb3a$^{+/+}$ Balb/c background strain)
Cell lines *in vitro* in clonogenic survival	Radioresistant
Fresh marrow - CFU-GEMM	Radioresistant
IL-3-dependent cell lines	Radioresistant
Marrow stromal cell lines	Radioresistant
Long-term marrow culture production of hematopoietic cells	Increased longevity
Survival of mice after TBI	Radioresistant
Level of antioxidant stores in cells	Increased
Stress response gene induction by radiation (RNA in irradiated cell lines *in vitro*)	Increased MnSOD Increased p21 Decreased TGF-β Decreased p53
Stress response induced proteins in plasma after TBI	Decreased Eotaxin Decreased G-CSF Decreased IL-6 Decreased MCP-1
Level of apoptosis induced by radiation	Decreased

FIG. 10.

Panel A: A potential signaling network that mediates the radioresistance of Serpinb3a$^{-/-}$ mice and cell lineages upregulated and downregulated pathways contributing to radioresistance. Panel B: Summary of *in vitro* and *in vivo* data consistent with the oxidative-stress-resistant phenotype of Serpinb3a$^{-/-}$ mice and cell lines.